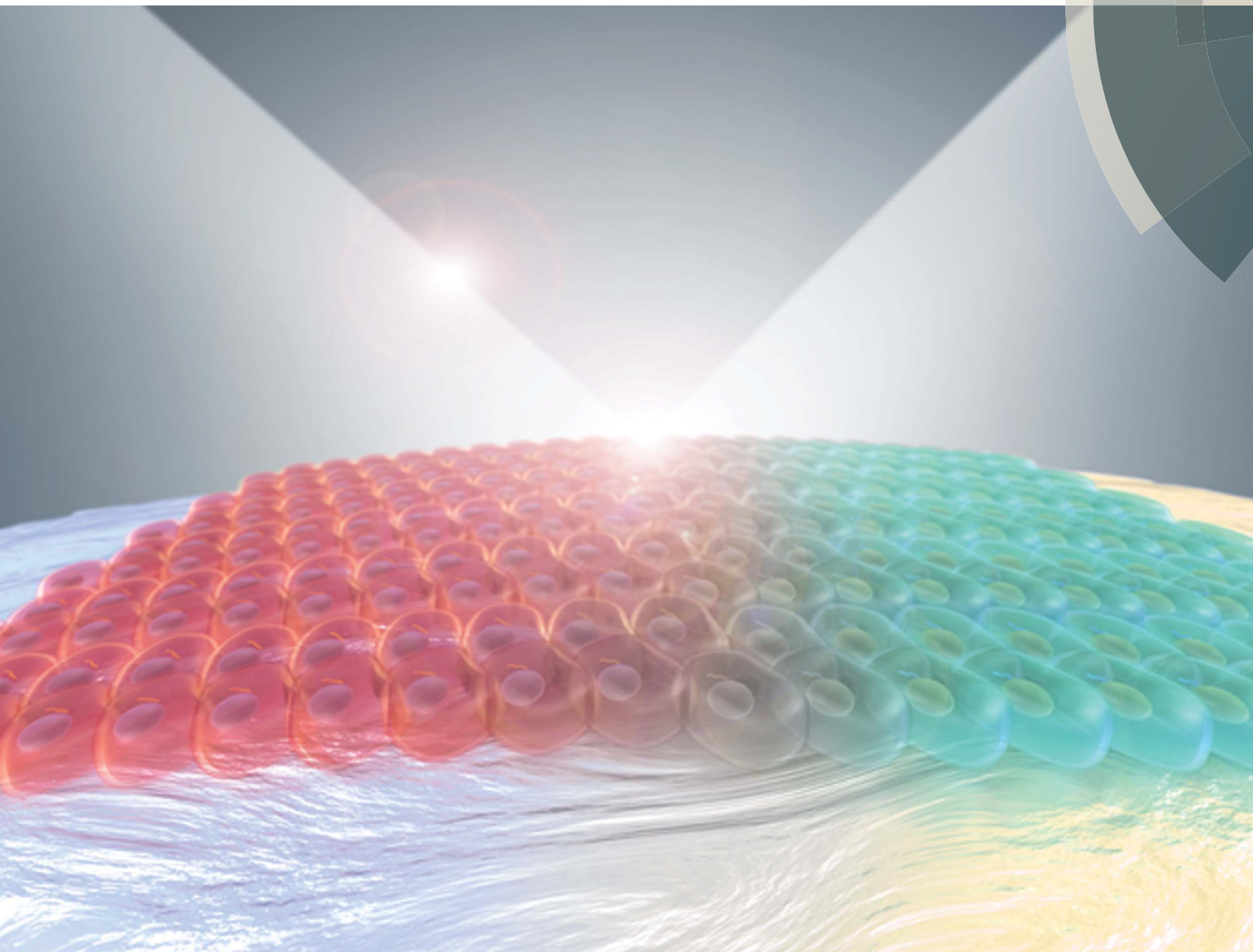


# Analytical Methods

[www.rsc.org/methods](http://www.rsc.org/methods)



ISSN 1759-9660



**COMMUNICATION**

Francis L. Martin, Matthew Briggs *et al.*  
Aluminium foil as a potential substrate for ATR-FTIR, transfection FTIR or Raman spectrochemical analysis of biological specimens

**175**  
YEARS

CrossMark  
click for updatesCite this: *Anal. Methods*, 2016, 8, 481Received 4th October 2015  
Accepted 30th October 2015

DOI: 10.1039/c5ay02638e

[www.rsc.org/methods](http://www.rsc.org/methods)

The substantial cost of substrates is an enormous obstacle in the successful translation of biospectroscopy (IR or Raman) into routine clinical/laboratory practice (screening or diagnosis). As a cheap and versatile substrate, we compared the performance of readily available aluminium (Al) foil with low-E, Au-coated and glass slides for cytological and histological specimen analysis by attenuated total reflection Fourier-transform infrared (ATR-FTIR), transfection FTIR or Raman spectroscopy. The low and almost featureless background signal of Al foil enables the acquisition of IR or Raman spectra without substrate interference or sacrificing important fingerprint biochemical information of the specimen, even for very thin samples with thicknesses down to 2  $\mu\text{m}$ . Al foil is shown to perform as well as, if not better than, low-E or Au-coated slide, irrespective of its relatively rough surface. Although transmission FTIR is not possible on Al foil, this work demonstrates Al foil is an inexpensive, readily available and versatile substrate suitable for ATR-FTIR, transfection FTIR or Raman spectrochemical measurements of diverse biological specimens. The features of Al foil demonstrated here could promote a transition towards accessible substrates that can be readily implemented in either research or clinical settings.

## Introduction

Vibrational spectroscopies including infrared (IR) or Raman have become highly regarded techniques for biological/ biomedical applications through many proof-of-concept studies. Due to their fingerprinting capability, they could play a significant role in histopathology, cytology, targeting biopsies, determining surgical margins, treatment, monitoring and drug studies.<sup>1–12</sup> However, successful translation and implementation of such techniques into routine clinical or laboratory practice has been slow, as recurrent costs of substrates represent a significant challenge.

<sup>a</sup>Key Laboratory of Urban Pollutant Conversion, Institute of Urban Environment, Chinese Academy of Sciences, Xiamen 361021, China

<sup>b</sup>Centre for Biophotonics, Lancaster Environment Centre, Lancaster University, Lancaster LA1 4YQ, UK. E-mail: [lcui@iue.ac.cn](mailto:lcui@iue.ac.cn); [f.martin@lancaster.ac.uk](mailto:f.martin@lancaster.ac.uk)

# Aluminium foil as a potential substrate for ATR-FTIR, transfection FTIR or Raman spectrochemical analysis of biological specimens

Li Cui,<sup>\*ab</sup> Holly J. Butler,<sup>b</sup> Pierre L. Martin-Hirsch<sup>b</sup> and Francis L. Martin<sup>\*b</sup>

Many proof-of-concept studies have been conducted under optimal experimental conditions, using spectral-optimized but costly substrates to minimize substrate interference and maximize signal.<sup>3,13</sup> In transmission Fourier-transform IR (FTIR) measurements, IR transparent materials including  $\text{CaF}_2$ ,  $\text{BaF}_2$  and  $\text{ZnSe}$  slides are commonly used,<sup>14,15</sup> but have the disadvantages that they are both expensive and fragile, and thus unsuitable for routine applications. Transfection FTIR and attenuated total reflection (ATR)-FTIR configurations using highly IR reflective low-E or Au (Ag)-coated slides may give a relatively low-cost alternative, but these still greatly exceed the current costs for glass slides alone.<sup>1,14,16,17</sup> For Raman measurements,  $\text{CaF}_2$  or Au (Al)-coated slide substrates without obvious background fluorescence and Raman signal are frequently used.<sup>1,7,18–20</sup>

In the routine clinical/laboratory environment that requires a high throughput procedure for enormous numbers of specimens, such as cervical screening, standard glass microscope slides are used as a substrate. However, glass slides are generally unsuitable for either IR or Raman spectral measurement, since one then needs to sacrifice the most important fingerprint region required for spectral discrimination and disease diagnosis, due to the strong IR absorption or fluorescence bands of glass.<sup>7</sup> This means that access to a broader spectrum can only be provided by more costly substrates. Additionally, the requirement for sample archiving in clinical practice implies that substrates are not reusable. Thus, for translation of biospectroscopy techniques for routine screening and/or diagnosis, a substrate without background signal interference and as inexpensive as glass is a major requirement.<sup>21</sup>

Ideally, spectroscopic diagnostic techniques should add in technical/medical value without compromising cost and/or efficiency. It is important to note that cost is not the single limiting factor for clinical/biological implementation, as a technique proven to improve quality of biological interpretation may justify increased expenditure. However, any substantial increase in running cost will not aid in the drive for clinical translation. To promote the translation of biospectroscopy to



practical clinical diagnosis, the search for a cheap, easily available, and robust substrate suitable for both IR or Raman measurement is an urgent consideration. In this regard, aluminium (Al) foil could be a potential alternative. Similar to other pure metals-based substrates such as Au (Ag, Al)-coated slides, low spectral background and lack of spectral features can be anticipated on Al foil. More importantly, Al foil has substantially low cost. For instance, an annual cost of only £4900 is estimated for cervical smear, biopsies and histology specimens in UK, which is only 1/350 that of glass slides in terms of cost (Table 1). To demonstrate the feasibility of Al foil, its performance in ATR-FTIR, transfection FTIR or Raman spectrochemical analysis of cytology and histology specimen was compared with other well-recognized substrates, *i.e.*, Au-coated, low-E and glass slides.

## Materials and methods

### Substrates

Four types of substrates were used herein, including Al foil (Kitchen quality, Terinex Limited, UK), Au-coated slides (Item no. AU. 0500, ALSI, Platypus Technologies), low-E slides (Kevley Technologies, USA) and glass slides (Thermo Scientific). Al foil was placed onto glass slides and fixed by some tape to facilitate ease of handling and archiving.

### Cell culture

An amphibian (A6) cell line was grown in modified L-15 medium supplemented with 70% Leibovitz's media (Gibco, Life Technologies Ltd, UK), 10% foetal bovine serum (Gibco), 1% penicillin ( $100 \text{ U mL}^{-1}$ ) and streptomycin ( $100 \mu\text{g mL}^{-1}$ ) (Cat no. DE17-603 E, Lonza group Ltd., Belgium) and 19% autoclaved MilliQ water in air at room temperature. A6 cells were routinely cultured in T75 flasks and harvested when confluent by disaggregating cells using 3 mL trypsin ( $170 \text{ U mL}^{-1}$ )/EDTA (0.02%) solution (Cat no. BE17-161E, Lonza group Ltd., Belgium) followed by neutralization using 7 mL modified L-15 medium.

To prepare fixed cell pellets on substrates, harvested A6 cells were centrifuged at 1000 rpm for 5 min to remove medium and then fixed in 70% ethanol (EtOH) for 1 h. After centrifugation and washing two more times using 70% EtOH, the final concentrated cells were applied to different substrates and air-dried.

To grow cells directly on substrates, substrates were initially sterilized by immersing in 70% EtOH and rinsed with autoclaved MilliQ water; then 2 mL harvested cells were seeded in

six-well plates containing substrates and to each an additional 4 mL modified L-15 medium was added. After two days of culture to allow cells to reach confluence, medium was removed and 70% EtOH was added for 1 h to fix, followed by washing in 70% EtOH twice more, whereupon substrates were left to air-dry.

### Tissue

A formalin-fixed, paraffin-embedded (FFPE) prostate tissue block was obtained. All experimental protocols for the use of archival tissue retrieved from the Royal Preston Hospital Research Tissue Bank were approved by the UK National Research Ethics Service (<http://www.hra.nhs.uk/about-the-hra/our-committees/nres/>; Research Ethics Committee reference: 10/H0308/75). A ribbon of 20  $\mu\text{m}$ -thick sections was cut by a microtome (Surgipath Medical Industries Inc), floated into a heated water bath at 40–50 °C, and finally picked up on substrates. After drying overnight, tissue slides were de-waxed by immersing in fresh xylene (histological grade, Sigma-Aldrich) for 2 min at room temperature; this process was repeated twice more. Subsequently, tissue slides were immersed in 100% fresh EtOH for 15 min twice and then to 70% fresh EtOH for 15 min twice. Fresh EtOH was used each time. Finally, tissue slides were allowed to air-dry prior to analysis.<sup>5</sup>

### ATR-FTIR spectroscopy

ATR-FTIR spectral measurements were performed using a Bruker TENSOR 27 FTIR spectrometer (Bruker Optics Ltd., Coventry, UK) with Helios ATR attachment containing a diamond crystal internal reflective element and a 45° incidence angle of IR beam. The ATR crystal was cleaned using MilliQ water and a new background spectrum was collected prior to analysis of a new sample. The instrument was set up to perform a total of 32 scans with  $8 \text{ cm}^{-1}$  spectral resolution on both background and sample. The sampling aperture of the system was  $250 \mu\text{m} \times 250 \mu\text{m}$ , and the mirror velocity was 2.2 kHz; it is a single signal bounce instrument and uses a diamond waveguide.

### Transfection FTIR spectroscopy

Transfection FTIR spectroscopy was conducted using a Nicolet Continuum FTIR Microscope (Thermo Scientific) with IR beam provided by a Nicolet 6700 FTIR spectrometer. A 15 $\times$  infinity reflachromat objective with numerical aperture of 0.58 was used to illuminate sample and collect signal from a sample aperture

**Table 1** Comparison of substrates price and estimated total annual cost of substrates in biomedical specimen screening in UK<sup>27–30</sup>

Substrates	Price per piece (£)	Annual cost of cervical smear (million £)	Annual cost of biopsies (million £)	Annual cost of histology (million £)	Total (million £)
CaF <sub>2</sub> (76.0 × 26.0 × 1.0 mm)	73.08	711.04	189.61	101.12	1001.78
Au-coated slide (75.0 × 25.0 × 0.7 mm)	42.08	409.46	109.19	58.23	576.88
Low-E (75.0 × 25.0 × 1.0 mm)	1.51	14.71	3.92	2.09	20.72
Glass (76.0 × 26.0 × 1.0 mm)	0.12	1.22	0.32	0.17	1.73
Aluminum foil (76.0 × 26.0 mm)	0.0004	0.0035	0.0009	0.0005	0.0049



of  $100 \times 100 \mu\text{m}$ . A total of 256 scans with spectral resolution of  $8 \text{ cm}^{-1}$  was setup for both background and sample collection.

### Raman spectroscopy

Raman spectroscopy was acquired using a Renishaw InVia confocal micro-Raman system (Renishaw, Gloucestershire, UK) equipped with a 100 mW 785 nm laser and  $1200 \text{ g mm}^{-1}$  grating. A  $100\times$  objective with numerical aperture of 0.85 was used to focus laser beam and collect Raman signal with an acquisition time of 30 s.

## Results and discussion

Three typical biological specimens were prepared, *i.e.*, EtOH-fixed cell pellet applied to substrates, cells grown directly on substrates and de-waxed prostate tissue section floated on substrates. Fig. 1 shows the optical images of different sample preparations. Fixed-cell pellets were more spherical and smaller than cells grown directly on substrates (Fig. 1a), which exhibited a more expansive shape, thus looking bigger but being much thinner than the fixed-cell pellet (Fig. 1b). In addition, compared with the smooth surface of Au-coated, low-E or glass slides, the shiny side of Al foil used herein is rougher. The non-shiny side of foil was even rougher and thus not used, considering its low reflectivity. The thin layers of cells grown directly on the rough foil were not as discernible as those on smooth Au-coated or low-E substrates (Fig. 1b). However, after ATR-FTIR diamond pressure, the foil became smoother due to its ductility and cells can be clearly observed on it. This also indicates a simple way to obtain a smooth foil, which may be needed for some samples requiring an optimal focus and thus a better signal. Tissue sections with a thickness of  $20 \mu\text{m}$  picked on substrates required de-waxing before measurement. De-waxing was performed by immersing and transferring tissue sections to different organic solvents of xylene, 100% EtOH, and 70% EtOH.<sup>5</sup> This process may cause tissue section detaching from substrates. Fig. 1c indicates that the rough surface of foil can hold and stick such tissue sections as well as on the smooth low-E slide.

ATR-FTIR spectra were first obtained from four blank substrates (Fig. 2). In the fingerprint region, from 900 to 1800

$\text{cm}^{-1}$  that is often most important for spectral discrimination and disease diagnosis, the Au-coated slide was cleanest without any obvious characteristic IR absorption band, followed by Al foil, which only showed a small band at  $950 \text{ cm}^{-1}$ . In comparison, a low-E slide displayed a moderately intense IR band at  $1120 \text{ cm}^{-1}$  whilst the glass slide spectrum exhibited multiple strong IR bands at  $960 \text{ cm}^{-1}$  and  $1400 \text{ cm}^{-1}$ . From ATR-FTIR spectra of a fixed-cell pellet, directly-grown cells and tissue section, only directly-grown cells consisting of a very thin layer exhibited spectral artefacts from the background signal of low-E ( $1120 \text{ cm}^{-1}$ ) and glass slides ( $960 \text{ cm}^{-1}$ ) (Fig. 2c), while the fixed-cell pellet and tissue section samples that were composed of a relatively thick layer displayed the same spectral features on all four substrates, indicating no interference from substrate background (Fig. 2b and d). This can be explained by the working principle of ATR-FTIR spectra. To generate ATR-FTIR spectra, the IR beam is directed through an internal reflection element (IRE) with a high refractive index (*e.g.*, diamond used here); the evanescent wave extending beyond the IRE surface penetrates the sample in direct contact with the IRE. The penetration depth of this wave typically ranges from 1 to  $2 \mu\text{m}$  within the  $1800\text{--}900 \text{ cm}^{-1}$  region but still with  $\sim 5\%$  intensity at a depth of  $3 \mu\text{m}$ .<sup>5</sup> So substrate interference can be avoided for samples thicker than  $2\text{--}3 \mu\text{m}$ , but for those  $< 2 \mu\text{m}$ , spectral artefacts from the underlying low-E or glass slide may become apparent, indicating that these substrates are unsuitable for thin samples. Bassan *et al.* also confirmed the interference of glass slide at sample thicknesses  $< 2 \mu\text{m}$  *via* both theoretical calculations and experimental ATR-FTIR measurements.<sup>22</sup> In comparison, the thin layer of cells grown directly on Al foil displayed similar spectral features to that on Au-coated slide. No obvious spectral artefacts were observed. This indicates the suitability of Al foil for preparations of very thin samples (*e.g.*,  $< 2 \mu\text{m}$ ) towards ATR-FTIR measurements; more importantly, foil is available at a much-reduced cost compared to Au-coated slides.

For the transfection FTIR sampling mode, measurements were conducted with an IR beam passing through the sample and reflecting back from the substrate (*i.e.*, the reflective surface) through the sample a second time.<sup>5</sup> Low-E slides are typical substrates used in transfection mode due to their high

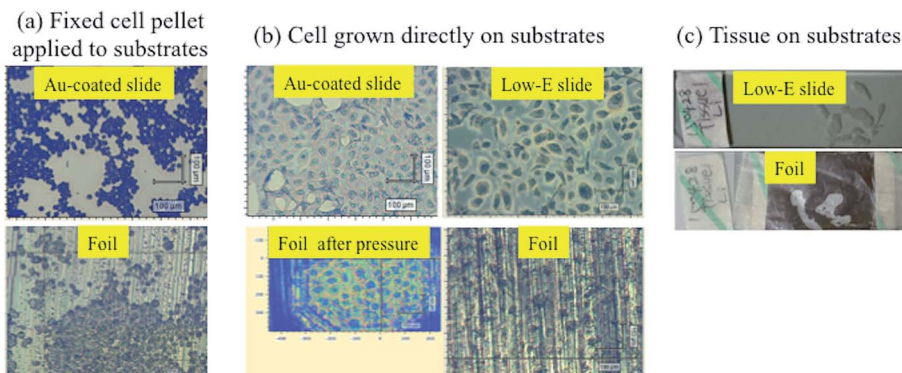


Fig. 1 Optical images of (a) fixed cell pellet; (b) directly-grown cells; and, (c) prostate tissue section on substrates.



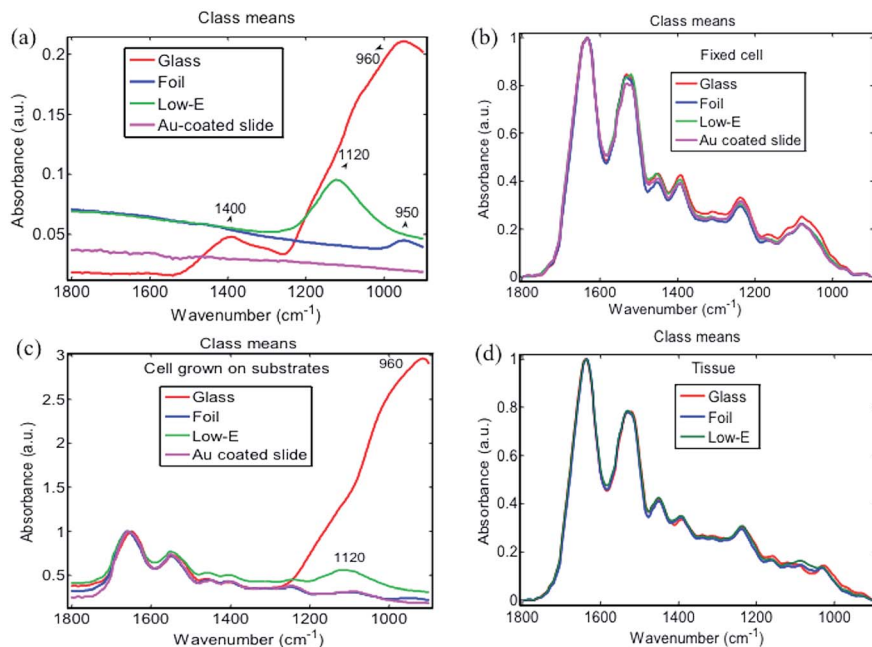


Fig. 2 ATR-FTIR spectra of (a) blank substrates; (b) fixed cell pellet; (c) cells directly grown on substrate; and, (d) prostate tissue section on substrate.

reflection towards IR beam combined with robustness and relatively low cost.<sup>14</sup> Background spectra from low-E, Au-coated slide and Al foil were similar (Fig. 3a), whereas glass displayed a very strong IR absorption from 800 to 1200 cm<sup>-1</sup> region due to the penetration of IR beam into glass lacking an IR-reflective coating. The strong absorption of glass severely influenced the sample spectra irrespective of whether the sample was a thick

fixed-cell pellet or thin layer of cells grown on glass (Fig. 3b). In contrast, spectra of fixed-cell pellets on low-E slides, Au-coated slides or Al foil displayed the same typical fingerprint features of cells without substrate interference (Fig. 3c). For the thin layer of cells grown on substrates, transfection FTIR spectra of cells were also obtained, but with a markedly lower signal-to-noise ratio (SNR) than fixed-cell pellets due to the sample thinness

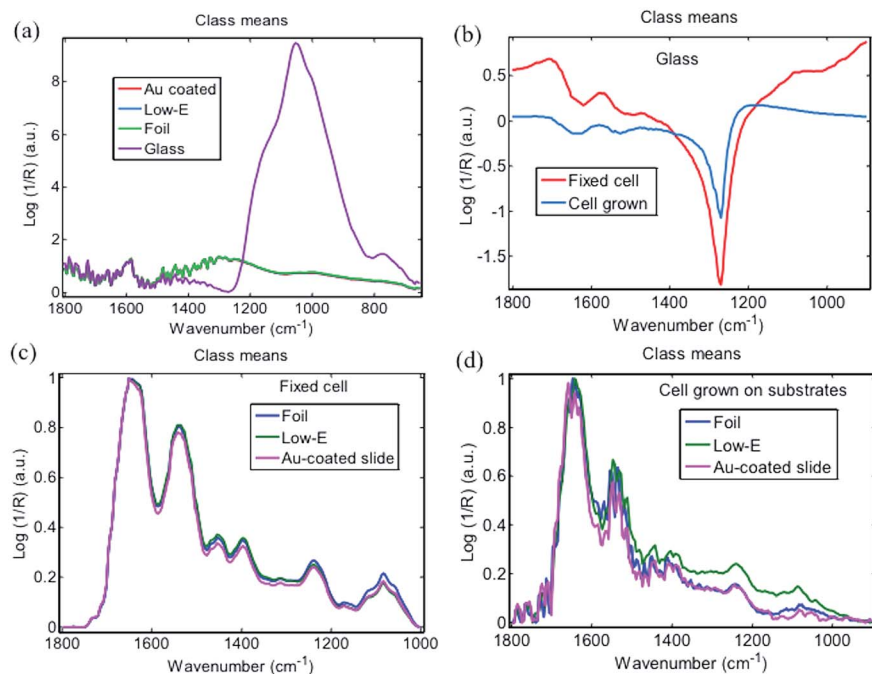


Fig. 3 Transfection FTIR spectra of (a) blank substrates; (b) fixed cell pellet or cells grown directly on glass; (c) fixed cell pellets on other substrates; and, (d) cells grown directly onto other substrates.



(Fig. 3d). This SNR was also lower than ATR-FTIR analysis of the same thin layer of cells grown on substrates (Fig. 2c), which should be related to the working principle of transfection and ATR mode.<sup>5</sup> These results indicate that IR beam reflection on Al foil is enough to obtain similar-quality transfection FTIR spectra as from low-E or Au-coated slides, despite the rougher surface than the latter. Therefore, Al foil is applicable for transfection FTIR mode with a lower cost than low-E slides. A comparison of the relative reflectivity of these substrates will be interesting.

Many recent publications demonstrate a non-linear spectral distortion in transfection FTIR spectroscopy caused by the electric field standing wave (EFSW).<sup>14,15,23–25</sup> This may result in spectral variation due to sample thickness rather than any biochemical differences. EFSW is suggested to be present on reflective metallic surfaces due to the interference of incident and reflected light. Smooth IR reflective low-E slides have been almost exclusively used to demonstrate the effect of EFSW; however, there is as yet no report studying the effect of substrate roughness on EFSW. On a rough surface like Al foil, reflected light may be emitted in many various directions different from the incident light. If this were the case, the probability of incident and reflected light interference, and how EFSW affects transfection FTIR spectra for samples mounted on a rough Al foil requires further study.

The performance of Al foil on Raman measurements was also investigated. Fig. 4a shows the raw Raman spectra of four blank substrates. Both low-E and glass display a strong and broad fluorescence band at  $1382\text{ cm}^{-1}$ .<sup>7,26</sup> In comparison, Al foil and Au-coated slide yield a very low and featureless spectral background. Raman spectra of three types of biomedical specimen on these substrates were also obtained. Unlike ATR- and transfection FTIR, all Raman spectra of the three biomedical specimens on low-E or glass slides exhibited interference from

the strong and broad glass band at  $1382\text{ cm}^{-1}$ , which severely masked the important fingerprint bands at  $1244$ ,  $1325$ ,  $1455\text{ cm}^{-1}$ , and even  $1650\text{ cm}^{-1}$  at the tail region of  $1382\text{ cm}^{-1}$ . This interference is more severe for the thin layer of cells grown directly on substrates, where no visible cell Raman bands can be observed over the strong background fluorescence of low-E or glass slides (Fig. 4c). This severe interference also makes it impossible to obtain biomedical specimen spectra by mathematically subtracting the glass band. Meanwhile, Raman spectra with all the well-defined bands constituting spectral fingerprints of cells or tissue are clearly distinguishable on Al foil or Au-coated slides, even for the thin layer of cells grown on substrates (Fig. 4b–d). Although the spectra of cells on Al foil were slightly tilting due to foil background compared with the rather flat spectra on Au-coated slide (Fig. 4c), it can be easily baseline subtracted without compromising any spectral features of cells (see inset of baseline-subtracted Raman spectra). Kamemoto *et al.* obtained high-quality near-IR Raman spectroscopy of cervical cancer tissue mounted on an Al-coated slides.<sup>7</sup> Athamneh *et al.* obtained Raman spectra of bacteria on Al foil.<sup>14</sup> These studies further confirm the wide applicability of Al substrate in various Raman analyses. In comparison, despite the relatively rougher surface of Al foil compared to Au-coated slides, advantages of low cost and minimal interference on spectral acquisition could make it a first choice for high throughput analyses.

Table 2 summaries the performance of Al foil and conventional substrates. Al foil performs as well as Au-coated slides in all ATR-FTIR, transfection FTIR or Raman spectrochemical measurements of very thin (cells grown directly on substrates) and thick specimens (fixed-cell pellet or tissue), but with a much reduced cost. In comparison, low-E is more suitable for ATR-FTIR measurement of samples thicker than  $3\text{ }\mu\text{m}$ , but not for

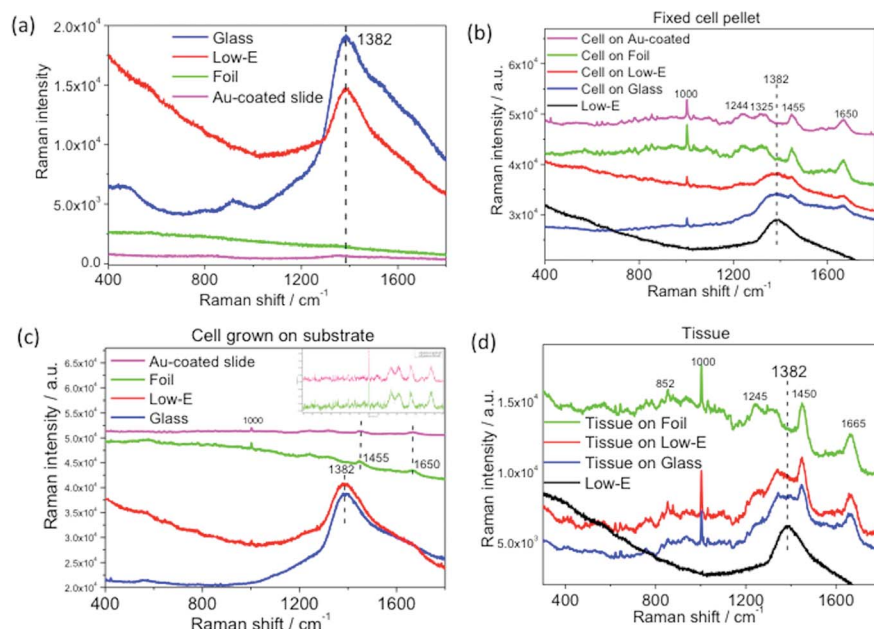


Fig. 4 Raman spectra of (a) blank substrates; (b) fixed cell pellet on substrates; (c) cells grown directly on substrates (inset represents baseline-subtracted Raman spectra on Au-coated slides or Al foil); and, (d) prostate tissue section on substrates.



Table 2 Performance and cost comparison of different substrates

Substrate	ATR-FTIR spectroscopy	Transflection FTIR spectroscopy	Raman spectroscopy	Cost
Au-coated slide	√	√	√	High
Low-E	√ (except for sample thinner than 2–3 μm)	√	×	Medium
Glass	×	×	×	Lower
Aluminum foil	√	√	√	Lowest

thinner specimens. Glass is cheap but unsuitable for either IR or Raman measurements because its strong background band will sacrifice the most important fingerprint biochemical information used for clinical diagnosis. Unfortunately, Al foil cannot be used in transmission FTIR because of its IR opacity.

Biocompatibility is an important consideration for future applications. A careful comparison indicates that ATR-FTIR spectral features of cells grown on Al foil are very close to other substrates including glass, low-E and Au-coated slide (Fig. 2c). Moreover, Raman spectra of cell grown on Al foil and Au-coated slide after baseline subtraction were almost identical (inset of Fig. 4c). These results may indicate that the biocompatibility of Al foil is comparable with conventional substrates. However, this will need to be assessed by conducting a comparison of survival rates of cells grown on such substrates.

## Conclusion

This study demonstrates that readily available and inexpensive Al foil can be used as a versatile and suitable substrate for preparing diverse cytology and histology specimens for ATR-FTIR, transflection FTIR or Raman spectroscopic measurements. The low and almost featureless background spectra of Al foil enable the acquisition of high-quality IR and Raman spectra without substrate interference or sacrificing important fingerprint biochemical information of biomedical specimen. It is also suitable for diverse specimens with a broader thickness ranging from less than 2 μm to above. These features together with its much lower cost and availability make Al foil a potential substrate for the future application of IR and Raman spectroscopy in biomedical diagnosis. Although there are still many things to consider towards achieving final implementation, such as clinical trials and adaptation to current instruments, the use of Al foil makes this process a step forward by providing an additional low-cost substrate option. With little additional cost, a slightly thicker Al foil could replicate typical slide dimensions to better allow for handling and archiving.

## Acknowledgements

This work was supported by China Scholarship Council, the National Natural Science Foundation of China (21173208), Natural Science Foundation of Ningbo (2014A610107) and Fujian Province (2015J01067).

## References

- M. Diem, A. Mazur, K. Lenau, J. Schubert, B. Bird, M. Miljkovic, C. Krafft and J. Popp, *J. Biophotonics*, 2013, **6**, 855–886.
- D. I. Ellis, D. P. Cowcher, L. Ashton, S. O'Hagan and R. Goodacre, *Analyst*, 2013, **138**, 3871–3884.
- C. Kendall, M. Isabelle, F. Bazant-Hegemark, J. Hutchings, L. Orr, J. Babrah, R. Baker and N. Stone, *Analyst*, 2009, **134**, 1029–1045.
- A. Nijssen, K. Maquelin, L. F. Santos, P. J. Caspers, T. C. B. Schut, J. C. D. Hollander, M. H. A. Neumann and G. J. Puppels, *J. Biomed. Opt.*, 2007, **12**, 034004.
- M. J. Baker, J. Trevisan, P. Bassan, R. Bhargava, H. J. Butler, K. M. Dorling, P. R. Fielden, S. W. Fogarty, N. J. Fullwood, K. A. Heys, C. Hughes, P. Lasch, P. L. Martin-Hirsch, B. Obinaju, G. D. Sockalingum, J. Sule-Suso, R. J. Strong, M. J. Walsh, B. R. Wood, P. Gardner and F. L. Martin, *Nat. Protoc.*, 2014, **9**, 1771–1791.
- F. L. Martin, J. G. Kelly, V. Llabjani, P. L. Martin-Hirsch, I. I. Patel, J. Trevisan, N. J. Fullwood and M. J. Walsh, *Nat. Protoc.*, 2010, **5**, 1748–1760.
- L. E. Kamemoto, A. K. Misra, S. K. Sharma, M. T. Goodman, H. Luk, A. C. Dykes and T. Acosta, *Appl. Spectrosc.*, 2010, **64**, 255–261.
- K. Kong, C. Kendall, N. Stone and I. Notingher, *Adv. Drug Delivery Rev.*, 2015, **89**, 121–134.
- J. Horsnell, C. Kallaway, C. Chan, J. Bristol and N. Stone, *Br. J. Surg.*, 2012, **99**, 5–6.
- K. Gajjar, L. D. Heppenstall, W. Y. Pang, K. M. Ashton, J. Trevisan, I. I. Patel, V. Llabjani, H. F. Stringfellow, P. L. Martin-Hirsch, T. Dawson and F. L. Martin, *Anal. Methods*, 2013, **5**, 89–102.
- A. I. M. Athamneh, R. A. Alajlouni, R. S. Wallace, M. N. Seleem and R. S. Senger, *Antimicrob. Agents Chemother.*, 2014, **58**, 1302–1314.
- L. Cui, P. Y. Chen, S. D. Chen, Z. H. Yuan, C. P. Yu, B. Ren and K. S. Zhang, *Anal. Chem.*, 2013, **85**, 5436–5443.
- L. T. Kerr, H. J. Byrne and B. M. Hennelly, *Anal. Methods*, 2015, **7**, 5041–5052.
- M. J. Pilling, P. Bassan and P. Gardner, *Analyst*, 2015, **140**, 2383–2392.
- D. Perez-Guaita, P. Heraud, K. M. Marzec, M. de la Guardia, M. Kiupel and B. R. Wood, *Analyst*, 2015, **140**, 2376–2382.
- I. Amenabar, S. Poly, W. Nuansing, E. H. Hubrich, A. A. Govyadinov, F. Huth, R. Krutokhvostov, L. B. Zhang, M. Knez, J. Heberle, A. M. Bittner and R. Hillenbrand, *Nat. Commun.*, 2013, **4**, 2890.
- J. Y. Li, R. Strong, J. Trevisan, S. W. Fogarty, N. J. Fullwood, K. C. Jones and F. L. Martin, *Environ. Sci. Technol.*, 2013, **47**, 10005–10011.
- D. Berry, E. Mader, T. K. Lee, D. Woebken, Y. Wang, D. Zhu, M. Palatinszky, A. Schintmeister, M. C. Schmid,



- B. T. Hanson, N. Shterzer, I. Mizrahi, I. Rauch, T. Decker, T. Bocklitz, J. Popp, C. M. Gibson, P. W. Fowler, W. E. Huang and M. Wagner, *Proc. Natl. Acad. Sci. U. S. A.*, 2015, **112**, E194–E203.
- 19 M. Q. Li, D. P. Canniffe, P. J. Jackson, P. A. Davison, S. FitzGerald, M. J. Dickman, J. G. Burgess, C. N. Hunter and W. E. Huang, *ISME J.*, 2012, **6**, 875–885.
- 20 S. A. Wang, J. H. Zhao, H. Lui, Q. L. He and H. S. Zeng, *Int. J. Spectrosc.*, 2010, **24**, 577–583.
- 21 [http://countrymeters.info/en/United\\_Kingdom\\_\(UK\)](http://countrymeters.info/en/United_Kingdom_(UK)), accessed 16 July 2015.
- 22 P. Bassan, A. Sachdeva, J. Lee and P. Gardner, *Analyst*, 2013, **138**, 4139–4146.
- 23 E. Staniszewska-Slezak, A. Rygula, K. Malek and M. Baranska, *Analyst*, 2015, **140**, 2412–2421.
- 24 J. Filik, M. D. Frogley, J. K. Pijanka, K. Wehbe and G. Cinque, *Analyst*, 2012, **137**, 853–861.
- 25 K. Kochan, P. Heraud, M. Kiupel, V. Yuzbasiyan-Gurkan, D. McNaughton, M. Baranska and B. R. Wood, *Analyst*, 2015, **140**, 2402–2411.
- 26 L. M. Fullwood, D. Griffiths, K. Ashton, T. Dawson, R. W. Lea, C. Davis, F. Bonnier, H. J. Byrne and M. J. Baker, *Analyst*, 2014, **139**, 446–454.
- 27 <http://www.crystran.co.uk/windows/calcium-fluoride-windows/calcium-fluoride-rectangular-windows>, accessed 16 July 2015.
- 28 <http://www.platypustech.com/glassslides.html>, accessed 16 July 2015.
- 29 <http://www.kevley.com/dnn/Ordering.aspx>, accessed 16 July 2015.
- 30 <http://www.scientificlabs.co.uk/product/MIC3022>, accessed 16 July 2015.

